

## PUBLISHED VERSION

Huang, David Mark; Sendner, Christian; Horinek, Dominik; Netz, Roland R.; Bocquet, Lyderic

[Water slippage versus contact angle: a quasiuniversal relationship](#) Physical Review Letters, 2008; 101(22):226101

©2008 American Physical Society

<http://link.aps.org/doi/10.1103/PhysRevLett.101.226101>

### PERMISSIONS

<http://publish.aps.org/authors/transfer-of-copyright-agreement>

“The author(s), and in the case of a Work Made For Hire, as defined in the U.S. Copyright Act, 17 U.S.C.

§101, the employer named [below], shall have the following rights (the “Author Rights”):

[...]

3. The right to use all or part of the Article, including the APS-prepared version without revision or modification, on the author(s)' web home page or employer's website and to make copies of all or part of the Article, including the APS-prepared version without revision or modification, for the author(s)' and/or the employer's use for educational or research purposes.”

10<sup>th</sup> May 2013

<http://hdl.handle.net/2440/65149>

## Water Slippage versus Contact Angle: A Quasiuniversal Relationship

David M. Huang,<sup>1,\*</sup> Christian Sendner,<sup>2</sup> Dominik Horinek,<sup>2</sup> Roland R. Netz,<sup>2</sup> and Lydéric Bocquet<sup>1,2,†</sup>

<sup>1</sup>*LPMCN, Université de Lyon, Université Lyon 1, and CNRS, UMR 5586, F-69622 Villeurbanne Cedex, France*

<sup>2</sup>*Physik Department, Technische Universität München, 85748 Garching, Germany*

(Received 24 June 2008; published 25 November 2008)

Using molecular dynamics simulations of an atomistic water model, we study the interfacial hydrodynamic slippage of water at various hydrophobic surfaces, both organic (silane monolayers) and inorganic (diamondlike and Lennard-Jones models). The measured slip lengths range from nanometers to tens of nanometers. Slip lengths on different surfaces are found to collapse nearly onto a single curve as a function of the static contact angle characterizing the surface wettability, thereby suggesting a quasiuniversal relationship. This dependence is rationalized on the basis of a simple scaling description of the fluid-solid friction at the microscopic level. The link between slippage and water depletion at hydrophobic surfaces is clarified. These results shed light on the controversy over experimental measurements of the slip length at smooth hydrophobic surfaces.

DOI: 10.1103/PhysRevLett.101.226101

PACS numbers: 68.08.-p, 47.15.G-, 68.15.+e, 68.35.Md

Understanding fluid flow on the nanoscale is relevant to many areas, from designing microfluidic devices [1,2] to comprehending transport through biological membrane channels [3]. An inherent feature of fluid flow through micro- and nanosized channels is the importance of interfacial effects, due to the high ratio of solid surface to fluid volume. In recent years, it has become clear that the no-slip (i.e., zero interfacial fluid velocity) boundary condition (BC) of macroscopic hydrodynamic theory does not necessarily hold at the nanoscale [4,5]. Instead, the fluid velocity  $\mathbf{v}$  at the surface is more appropriately described by a partial slip BC that relates the fluid velocity  $\mathbf{v}$  at the surface to its gradient  $\partial\mathbf{v}/\partial z$  in the direction normal to the surface by  $\mathbf{v} \equiv b(\partial\mathbf{v}/\partial z)$ , where  $b$  is the slip length [5].

The practical importance of fluid slippage has begun to be recognized in various domains, from microfluidics and biofluid dynamics to lubrication. In microfluidics, interfacial slip can be beneficial in reducing viscous friction at the surfaces and amplifying flow rates in pressure-driven flows [5]. The effect can be enormous for electrically driven flows (electro-osmosis), for which slip lengths in the nanometric range are sufficient to considerably enhance flow [6,7]. Such slip-induced amplifications are particularly relevant in the context of electrical energy conversion [8,9]. In water-transporting aquaporin membrane channels, the minimal interaction between water and the mostly hydrophobic channel surface is believed to be responsible for their high water permeability [10], and understanding interfacial slip could help elucidate the mechanisms by which these biological channels function. The appearance of slip at hydrophobic surfaces has a counterpart in the dynamics of biomolecules: Molecular dynamics (MD) simulations have shown that peptides have a high lateral mobility when adsorbed on a hydrophobic surface [11].

Since nanoscale fluid flow depends sensitively on the slip length, a good understanding of flow on these length

scales depends imperatively on accurate estimates or measurements of this quantity. But the scatter in the experimental data reported for the slip length of typical hydrophobic surfaces is enormous: For smooth hydrophobic surfaces (i.e., surfaces that are smooth on length scales larger than the solid lattice spacing), slip lengths spanning several orders of magnitude have been measured, even for apparently similar systems (generally, water on surfaces coated with alkylsilanes), ranging from nanometers [12–17] all the way up to micrometers [18,19]. It has been posited that the larger measured values of the slip length, rather than being intrinsic properties of the surface, are due to dissolved gas adsorption at the interface [20–22], and molecular dynamics simulations of a model Lennard-Jones (LJ) system have shown an increase in slip due to this phenomenon [23]. Slip lengths larger than a micron can be achieved but only with hydrophobic surfaces that are topographically structured on length scales larger than the atomic scale, the so-called superhydrophobic surfaces [24].

In this Letter, we perform nonequilibrium MD simulations of the SPC/E rigid simple point charge model [25] of water by applying shear boundary conditions and measure the slip length of water at various realistic hydrophobic surfaces. The goal is to provide insight into the influence of surface properties on water slippage, in order to resolve the controversy in the experimental literature. In this context, there is a strong need for firmly grounded numerical results using realistic water on atomistically modeled surfaces, thereby capturing the specific nature of water's behavior. Indeed, almost all published simulation studies of interfacial slip at nonwetting surfaces have looked at model LJ fluids [5,26], and very few simulation studies have measured the slip length for water at realistic surfaces, with the exception of a study of water flow around carbon nanotubes [27]. One key result of the present study is that all

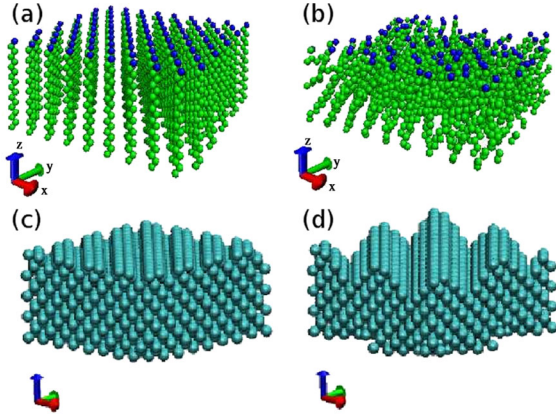


FIG. 1 (color online). Snapshots of some of the surfaces studied: (a) rigid alkylsilane chains, OPLS-UA (optimized potentials for liquid simulations-united atom [28]) model, in a hexagonal configuration with surface density  $\rho_{\text{surf}} = 4.0$  chains/nm<sup>-2</sup> (green: CH<sub>2</sub>; blue: CH<sub>3</sub>); (b) flexible alkylsilane chains (OPLS-UA model) with base atoms fixed in a hexagonal configuration with surface density  $\rho_{\text{surf}} = 4.0$  chains/nm<sup>-2</sup>; (c) diamond surface; (d) rough diamond surface (SD) with carbon atoms down to the fourth topmost layer removed.

results for the slip length  $b$  of water over various surface types collapse almost onto a single curve, suggesting a quasiuniversal dependence of the slip length  $b$  on the contact angle  $\theta_c$ . The measurements are consistent with a simple scaling relationship of the form  $b \propto (1 + \cos\theta_c)^{-2}$ , in agreement with a simple theoretical picture.

Two different classes of hydrophobic surfaces were studied: organic surfaces ( $n$ -alkylsilane monolayers) and inorganic surfaces [diamond (100) surface and model (100) surfaces composed of close-packed lattices of LJ atoms]. A few examples of the surfaces considered are depicted in Fig. 1. The whole set of studied surfaces is summarized in Table I in the supplementary information [28]. In all simulations, several thousand SPC/E [25] water molecules were used. Equilibrium MD simulations were performed to measure static interfacial quantities (water interfacial profiles, surface tension, and contact angles), while nonequilibrium Couette flow simulations, as sketched in Fig. 2, allowed the slip length on the various surfaces to be measured [28]. Technical details concerning the simulations performed can be found in the supplementary information [28].

Figure 3 shows all of our results for the different surfaces in terms of the slip length  $b$  as a function of the contact angle  $\theta_c$ . For contact angles  $\theta_c$  all the way up to roughly 150°, the slip length  $b$  does not exceed 20 nm. These results are in accord with some recent experimental measurements of  $b$  for surfaces of this type [12,14–17] but call into question other results, which have measured slip lengths on the order of micrometers [18,19].

All of the points in Fig. 3 are seen to lie roughly on a universal curve  $b(\theta_c)$ . While the collapse is not perfect,

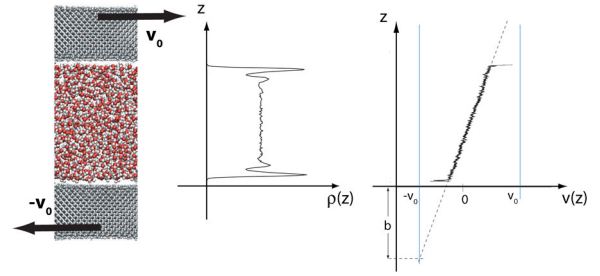


FIG. 2 (color online). Sketch of water density  $\rho(z)$  and flow profile  $v(z)$  close to hydrophobic surfaces that are sheared at velocity  $v_0$ . The slip length  $b$  is defined as the extrapolation length for the velocity profile, i.e., the distance from the interface at which the fluid velocity equals the surface velocity. A thin depletion layer in the water density profile is exhibited close to the hydrophobic surfaces.

such a result is not *a priori* expected—and is particularly intriguing—notably, in view of the range of surface characteristics (e.g., solid density, roughness, and “commensurability” of the solid lattice and liquid molecules) gathered in this plot.

Furthermore, a scaling formula  $b(\theta_c) \propto (\cos\theta_c + 1)^{-2}$  can be proposed on the basis of a simple argument. The slip length  $b$  is related to the solid-liquid friction coefficient  $\lambda$ , as  $b = \eta/\lambda$ , with  $\eta$  the shear viscosity [5]. As with any dissipation coefficient, a Green-Kubo formula can be obtained for  $\lambda$ , in the form  $\lambda = \frac{1}{Sk_B T} \int_0^\infty dt \langle F_x(t) \cdot F_x(0) \rangle$ , with  $F_x$  the total lateral force acting on the surface with area  $S$ ; the average is taken over equilibrium configurations

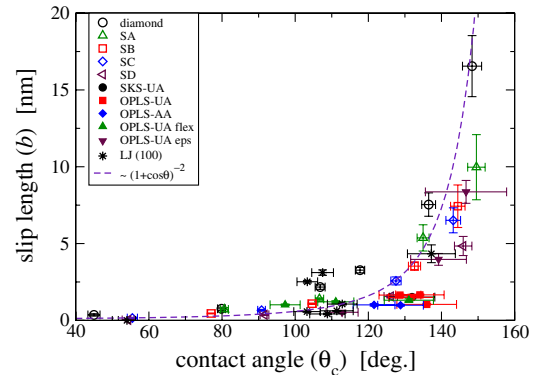


FIG. 3 (color online). Water slip length  $b$  as a function of contact angle  $\theta_c$  for all studied surfaces. The dashed line is a scaling function of the form  $b(\theta_c) \propto (\cos\theta_c + 1)^{-2}$ . The surfaces are (1) diamondlike surfaces [diamond ( $\circ$ ), rough diamond SA ( $\triangle$ ), rough diamond SB ( $\square$ ), rough diamond SC ( $\diamond$ ), rough diamond SD ( $\blacktriangleleft$ )]; (2) surfaces made of alkylsilane chains, using both SKS (Smit-Karabomi-Siepmann [28]) and OPLS models [SKS-UA (united atoms) ( $\bullet$ ), OPLS-UA ( $\blacksquare$ ), OPLS-AA (all atom) ( $\blacklozenge$ ), flexible OPLS-UA model ( $\blacktriangle$ ), OPLS-UA model with varying liquid-solid interactions ( $\blacktriangledown$ )]; (3) Lennard-Jones (100) surfaces (\*). See the supplementary information [28] for further simulation details on the studied surfaces.

[5,26]. An order of magnitude estimate for  $\lambda$  is then obtained by approximating the force autocorrelation function by  $\int_0^\infty dt \langle F_x(t) \cdot F_x(0) \rangle \approx \langle F_x^2 \rangle \cdot \tau$ , where  $\langle F_x^2 \rangle$  is the mean squared surface force at equilibrium, and the relaxation time scale  $\tau$  is given typically by a diffusion time over a microscopic lateral scale  $\sigma$  of the surface:  $\tau \sim \sigma^2/D$ , with  $D$  the fluid diffusion coefficient. The main dependence of  $\lambda$  on the fluid-solid interaction thus comes from the mean squared interaction force  $\langle F_x^2 \rangle$  between the fluid and the solid, which on dimensional grounds is expected to scale like  $\langle F_x^2 \rangle \propto (\varepsilon_{sf}/\sigma^2)^2 S$ , where  $\varepsilon_{sf}$  is the LJ fluid-solid energy parameter. This predicts  $b = \eta/\lambda \propto \varepsilon_{sf}^{-2}$ . Now, combining the Young equation and the Laplace estimate of the interfacial tensions in terms of the direct interaction energy between the liquid (or vapor) and the solid [29], the dependence of the static contact angle on the direct liquid-solid interactions can be obtained as  $\cos\theta_c + 1 \propto \varepsilon_{sf}$ . With  $b \propto \varepsilon_{sf}^{-2}$ , we thus predict the observed behavior  $b \propto (1 + \cos\theta_c)^{-2}$ . The scaling form predicted by this simple physically motivated argument is globally confirmed by the simulation results, as shown in Fig. 3, with deviations seen for rough surfaces. To our knowledge, no other microscopic theory exists to quantify the relationship between  $b$  and  $\theta_c$  for a complex fluid such as water; a complete theoretical treatment would be a formidable challenge but one that warrants further study.

It is interesting to investigate finally the relationship between slippage and water depletion at the surface. A classical, alternative, theory for the slip length considers the apparent slip due to fluid flow over a layer of gas of thickness  $\delta$  induced by the surface, giving  $b = \delta(\frac{\eta_l}{\eta_g} - 1)$ , where  $\eta_l$  and  $\eta_g$  are the liquid and gas viscosities, respectively [4,20]. This equation for  $b$  is commonly used to estimate the slip length from measurements of the width of the water depletion layer at the surface [22]. While this simple picture is appealing, it relies on the assumption that a gas viscosity can be defined in the molecular-sized depletion layer, a rather drastic and uncontrolled assumption (see, e.g., the inset in Fig. 4). We have thus measured the relationship between the slip length and the depletion layer width for diamond surfaces with varying  $\varepsilon_{sf}$ . The width  $\delta$  of the depletion layer is defined as an excess quantity for the density profile, according to  $\delta = \int_{-\infty}^\infty dz [1 - \rho_s(z)/\rho_s^b - \rho_f(z)/\rho_f^b]$  [30], where  $\rho_s(z)$  and  $\rho_f(z)$  are the densities of the solid and liquid, respectively, at position  $z$  and  $\rho_s^b$  and  $\rho_f^b$  are their respective bulk values. Results for the slip length versus the depletion layer width are shown in Fig. 4 for the three “smoothest” diamond surfaces (diamond, SA, and SB, for which the depletion layer can be defined unambiguously). As shown in this figure, no linear relationship is found between  $b$  and  $\delta$ , in contrast to the prediction of the simple two-layer model. Rather, a scaling relationship of  $b \propto \delta^4$  is found to fit the simulation data. Since  $b \propto (1 + \cos\theta_c)^{-2}$ , this scaling sug-

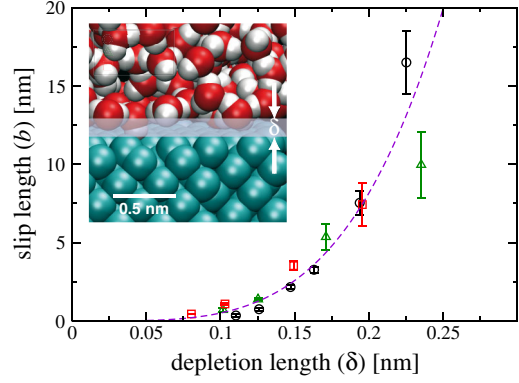


FIG. 4 (color online). Slip length  $b$  as a function of the water depletion length  $\delta$  for diamond surfaces (same symbols as in Fig. 3), with varying  $\varepsilon_{sf}$ . The depletion layer is calculated using the definition of Ref. [30]. The physical meaning of the depletion layer width  $\delta$  is sketched in the inset. The dashed line is the scaling prediction  $b \propto \delta^4$ .

gests that the depletion layer depends on the contact angle according to  $\delta^{-2} \propto (1 + \cos\theta_c)$ . Such a relationship is indeed consistent with the simulation data (see the supplementary information [28]) and reflects the effect of long-range interactions on the surface tension. Indeed, these effects can be estimated using the relation  $\gamma_{SL} = \gamma_{LV} + \gamma_{SV} + V_{SL}$  [31], where  $V_{SL}$  is the interaction energy for the liquid-solid interface, taking into account the existence of a depletion layer with finite width. Various terms may contribute to  $V_{SL}$ , in particular, van der Waals direct interactions, but also the Casimir fluctuation-induced interaction energy originating from the entropic loss of the fluctuating “vacuum” depletion layer at the solid surface [32]. Describing  $V_{SL}$  by a term of the form  $-A/\delta^2$ , where  $A$  is a Hamaker constant with  $A \sim k_B T$ , yields  $1 + \cos\theta_c \propto \frac{A}{\gamma_{LV}} \delta^{-2}$ , as verified numerically. This result suggests, however, that the corresponding Hamaker constant is independent of  $\varepsilon_{sf}$ , i.e.,  $A \propto \varepsilon_{sf}^0$ , thereby pointing to a nontrivial origin of the observed scaling. This simple description thus deserves further theoretical investigation, involving a full statistical treatment of the interface. Coming back to slippage effects, the combination of the two previous scalings  $b \propto (1 + \cos\theta_c)^{-2}$  and  $1 + \cos\theta_c \propto \delta^{-2}$  provides the proposed relationship  $b \propto \delta^4$ , consistent with the MD simulations (Fig. 4).

This nonlinear relationship between the slip length and the depletion layer width shows that the simple two-layer picture cannot account for the complexity of the slippage phenomenon. Conversely, Fig. 4 shows that the slip length is a very sensitive probe of water depletion at hydrophobic surfaces. In this context, it is interesting to note that, from a quantitative point of view, the slip lengths measured in the simulations do not exceed a few tens of nanometers: Numerically,  $b \sim 20$  nm for contact angles  $\theta_c \sim 140^\circ$ , while on the experimental side such values are typically measured for less hydrophobic surfaces, with contact an-

gles  $\sim 110^\circ$  [16,17]. Several hypotheses can be formulated to understand this fair agreement. The strong dependence of the slip length on the depletion layer width is a first one. The depletion layer measured experimentally for silanized surfaces [22] is indeed slightly larger than that obtained in the simulations (typically by a few angstroms): As seen in Fig. 4, this slight underestimate in MD simulations may be responsible for the missing factor between the experimental and the simulated slip length. Another related hypothesis is the role of dissolved gases on slippage, put forward in various works [20–23]. Experimentally, the depletion layer has been measured to increase substantially with the dissolved gas content [22], a fact which, in line with Fig. 4, would also help to reconcile the experimental and numerical values for the slip length. Further numerical work would be required to explore the role of dissolved gas, in line with the simulations of Ref. [23], but using realistic models for water and the surfaces, as has been done in the present study.

In conclusion, we have used molecular dynamics simulations of a realistic water model to study the slippage of water on various types of smooth hydrophobic surfaces. We have shown that the contact angle is the crucial parameter controlling water slippage, with results for the slip length versus the contact angle on many different types of surfaces collapsing onto a nearly universal curve. Typical values of the slip length range from a few nanometers up to tens of nanometers, in agreement with the most recent experiments [12–17]. A strong dependence of slippage on water depletion at the surface has been found, pointing to an intimate link between the static and dynamic characteristics of the surface. These results shed light on the controversy in the experimental literature over the magnitude of water slippage at hydrophobic surfaces, for which an enormous range of values have been measured.

This work was supported by ANR pNANO, by NIM, and by the Elitenetzwerk Bayern in the framework of CompInt. L. B. thanks Jens Eggers for fruitful discussions on the subject. L. B. acknowledges support from the von Humboldt foundation.

---

\*Present address: Chemical Engineering and Material Science Department, University of California, Davis, CA 95616, USA.

†Corresponding author.

lyderic.bocquet@univ-lyon1.fr

- [1] H. A. Stone, A. D. Stroock, and A. Ajdari, *Annu. Rev. Fluid Mech.* **36**, 381 (2004).
- [2] T. M. Squires and S. R. Quake, *Rev. Mod. Phys.* **77**, 977 (2005).
- [3] B. L. de Groot and H. Grubmüller, *Curr. Opin. Struct. Biol.* **15**, 176 (2005).
- [4] E. Lauga, M. P. Brenner, and H. A. Stone, *Microfluidics: The No-Slip Boundary Condition* (Springer, New York, 2005), Chap. 15.
- [5] L. Bocquet and J.-L. Barrat, *Soft Matter* **3**, 685 (2007).
- [6] V. M. Muller, I. P. Sergeeva, V. D. Sobolev, and N. V. Churaev, *Colloid J. USSR* **48**, 606 (1986).
- [7] L. Joly *et al.*, *Phys. Rev. Lett.* **93**, 257805 (2004); C. I. Bouzigues, P. Tabeling, and L. Bocquet, *ibid.* **101**, 114503 (2008).
- [8] S. Pennathur, J. C. T. Eijkel, and A. van der Berg, *Lab Chip* **7**, 1234 (2007).
- [9] Y. Ren and D. Stein, *Nanotechnology* **19**, 195707 (2008).
- [10] H. Sui *et al.*, *Nature (London)* **414**, 872 (2001).
- [11] D. Horinek *et al.*, *Proc. Natl. Acad. Sci. U.S.A.* **105**, 2842 (2008).
- [12] O. I. Vinogradova and G. E. Yakubov, *Langmuir* **19**, 1227 (2003).
- [13] P. Joseph and P. Tabeling, *Phys. Rev. E* **71**, 035303 (2005).
- [14] A. Maali, T. Cohen-Bouhacina, and H. Kellay, *Appl. Phys. Lett.* **92**, 053101 (2008).
- [15] C.-H. Choi, K. J. A. Westin, and K. S. Breuer, *Phys. Fluids* **15**, 2897 (2003).
- [16] C. Cottin-Bizonne, B. Cross, A. Steinberger, and É. Charlaix, *Phys. Rev. Lett.* **94**, 056102 (2005).
- [17] L. Joly, C. Ybert, and L. Bocquet, *Phys. Rev. Lett.* **96**, 046101 (2006).
- [18] Y. Zhu and S. Granick, *Phys. Rev. Lett.* **87**, 096105 (2001).
- [19] D. C. Tretheway and C. D. Meinhart, *Phys. Fluids* **14**, L9 (2002).
- [20] O. I. Vinogradova, *Langmuir* **11**, 2213 (1995).
- [21] P.-G. de Gennes, *Langmuir* **18**, 3413 (2002).
- [22] D. A. Doshi, E. B. Watkins, J. N. Israelachvili, and J. Majewski, *Proc. Natl. Acad. Sci. U.S.A.* **102**, 9458 (2005).
- [23] S. M. Dammer and D. Lohse, *Phys. Rev. Lett.* **96**, 206101 (2006).
- [24] P. Joseph *et al.*, *Phys. Rev. Lett.* **97**, 156104 (2006).
- [25] H. J. C. Berendsen, J. R. Grigera, and T. P. Straatsma, *J. Phys. Chem.* **91**, 6269 (1987).
- [26] J.-L. Barrat and L. Bocquet, *Phys. Rev. Lett.* **82**, 4671 (1999).
- [27] J. H. Walther, T. Werder, R. L. Jaffe, and P. Koumoutsakos, *Phys. Rev. E* **69**, 062201 (2004).
- [28] See EPAPS Document No. E-PRLTAO-101-025849 for simulation details and further results on the depletion layer. For more information on EPAPS, see <http://www.aip.org/pubservs/epaps.html>.
- [29] J. Rowlinson and B. Widom, *Molecular Theory of Capillarity* (Oxford University Press, Oxford, 1982), Chap. 1, pp. 4–9.
- [30] J. Janěček and R. R. Netz, *Langmuir* **23**, 8417 (2007).
- [31] P.-G. de Gennes, F. Brochard-Wyart, and D. Quéré, *Capillarity and Wetting Phenomena: Drops, Bubbles, Pearls, Waves* (Springer, New York, 2003).
- [32] M. Kardar and R. Golestanian, *Rev. Mod. Phys.* **71**, 1233 (1999).